

# Chalcogenide optical microwires cladded with fluorine-based CYTOP

LIZHU LI,\* NURMEMET ABDUKERIM, AND MARTIN ROCHETTE

Department of Electrical and Computer Engineering, 3480 University Street, McGill University, Montreal H3A 2A7, Canada

\*lizhu.li@mail.mcgill.ca

**Abstract:** We demonstrate optical transmission results of highly nonlinear  $\text{As}_2\text{Se}_3$  optical microwires cladded with fluorine-based CYTOP, and compare them with microwires cladded with typical hydrogen-based polymers. In the linear optics regime, the CYTOP-cladded microwire transmits light in the spectral range from 1.3  $\mu\text{m}$  up to  $>2.5 \mu\text{m}$  without trace of absorption peaks such as those observed using hydrogen-based polymer claddings. The microwire is also pumped in the nonlinear optics regime, showing multiple-orders of four-wave mixing and supercontinuum generation spanning from 1.0  $\mu\text{m}$  to  $>4.3 \mu\text{m}$ . We conclude that with such a broadband transparency and high nonlinearity, the  $\text{As}_2\text{Se}_3$ -CYTOP microwire is an appealing solution for nonlinear optical processing in the mid-infrared.

©2016 Optical Society of America

**OCIS codes:** (160.4330) Nonlinear optical materials; (160.4760) Optical properties; (160.5470) Polymers; (190.4410) Nonlinear optics, parametric processes; (220.0220) Optical design and fabrication.

## References and links

1. I. T. Sorokina and K. L. Vodopyanov, *Solid-State Mid-Infrared Laser Sources* (Springer Science and Business Media, 2003).
2. V. A. Serebryakov, É. V. Boïko, N. N. Petrishchev, and A. V. Yan, "Medical applications of mid-IR lasers. Problems and prospects," *J. Opt. Technol.* **77**(1), 6–17 (2010).
3. U. Willer, M. Saraji, A. Khorsandi, P. Geiser, and W. Schade, "Near- and mid-infrared laser monitoring of industrial processes, environment and security applications," *Opt. Lasers Eng.* **44**(7), 699–710 (2006).
4. G. P. Agrawal, *Nonlinear Fiber Optics* (Academic, 2007).
5. I. Breunig, D. Haertle, and K. Buse, "Continuous-wave optical parametric oscillators: recent developments and prospects," *Appl. Phys. B* **105**(1), 99–111 (2011).
6. A. Al-Kadry, M. El Amraoui, Y. Messaddeq, and M. Rochette, "Two octaves mid-infrared supercontinuum generation in  $\text{As}_2\text{Se}_3$  microwires," *Opt. Express* **22**(25), 31131–31137 (2014).
7. Amorphous materials, Inc., "AMTIR-2: Arsenic selenide glass  $\text{AsSe}$ ," and "AMTIR-6: Arsenic trisulfide glass  $\text{As}_2\text{S}_3$ ," <http://www.amorphousmaterials.com/products/>.
8. G. Lenz, J. Zimmermann, T. Katsufuji, M. E. Lines, H. Y. Hwang, S. Spälter, R. E. Slusher, S. W. Cheong, J. S. Sanghera, and I. D. Aggarwal, "Large Kerr effect in bulk Se-based chalcogenide glasses," *Opt. Lett.* **25**(4), 254–256 (2000).
9. P. Dumais, A. Villeneuve, P. G. J. Wigley, F. Gonthier, S. Lacroix, G. I. Stegeman, and J. Bures, "Enhanced self-phase modulation in tapered fibers," *Opt. Lett.* **18**(23), 1996–1998 (1993).
10. P. Russell, "Photonic crystal fibers," *Science* **299**(5605), 358–362 (2003).
11. E. C. Mägi, L. B. Fu, H. C. Nguyen, M. R. E. Lamont, D. I. Yeom, and B. J. Eggleton, "Enhanced Kerr nonlinearity in sub-wavelength diameter  $\text{As}_2\text{Se}_3$  chalcogenide fiber tapers," *Opt. Express* **15**(16), 10324–10329 (2007).
12. C. Baker and M. Rochette, "High nonlinearity and single-mode transmission in tapered multimode  $\text{As}_2\text{Se}_3$ -PMMA fibers," *IEEE Photonics J.* **4**(3), 960–969 (2012).
13. C. Baker and M. Rochette, "Highly nonlinear hybrid  $\text{AsSe}$ -PMMA microtapers," *Opt. Express* **18**(12), 12391–12398 (2010).
14. L. Li, A. Al-Kadry, N. Abdikerim, and M. Rochette, "Design, fabrication and characterization of PC, COP and PMMA-cladded  $\text{As}_2\text{Se}_3$  microwires," *Opt. Mater. Express* **6**(3), 912–921 (2016).
15. J. Workman, Jr. and L. Weyer, *Practical Guide to Interpretive Near-Infrared Spectroscopy* (CRC Press, 2007).
16. Y. Sun, S. Dai, P. Zhang, X. Wang, Y. Xu, Z. Liu, F. Chen, Y. Wu, Y. Zhang, R. Wang, and G. Tao, "Fabrication and characterization of multimaterial chalcogenide glass fiber tapers with high numerical apertures," *Opt. Express* **23**(18), 23472–23483 (2015).
17. Asahi Glass Co., "CYTOP," 2009. <http://www.agc.com/kagaku/shinsei/cytop/en/>.
18. J. Málek and J. Šhánělová, "Structural relaxation of  $\text{As}_2\text{Se}_3$  glass and viscosity of supercooled liquid," *J. Non-Cryst. Solids* **351**(43), 3458–3467 (2005).
19. D. M. Hoffman and A. L. Shields, "Rheological properties and molecular weight distributions of four perfluorinated thermoplastic polymers," *Polym. Prepr.* **50**(2), 156 (2009).
20. F. W. Billmeyer, *Textbook of Polymer Science* (John Wiley and Sons, 1984).

21. C. Stamboulides and S. G. Hatzikiriakos, "Rheology and processing of molten poly (methyl methacrylate) resins," *Int. Polym. Proc.* **21**(2), 155–163 (2006).
22. P.A. Bélanger, *Optical Fiber Theory: A Supplement to Applied Electromagnetism*, vol. 5 (World Scientific, 1993).
23. J. Nishii, T. Yamashita, and T. Yamagishi, "Chalcogenide glass fiber with a core-cladding structure," *Appl. Opt.* **28**(23), 5122–5127 (1989).
24. C. Baker and M. Rochette, "A generalized heat-brush approach for precise control of the waist profile in fiber tapers," *Opt. Mater. Express* **1**(6), 1065–1076 (2011).
25. J. M. Dudley and J. R. Taylor, *Supercontinuum Generation in Optical Fibers* (Cambridge University Press, 2010).
26. T. A. Cerni, "An infrared hygrometer for atmospheric research and routine monitoring," *J. Atmos. Oceanic Technol.* **11**(2), 445–462 (1994).
27. A. Al-Kadry, L. Li, M. El Amraoui, T. North, Y. Messaddeq, and M. Rochette, "Broadband supercontinuum generation in all-normal dispersion chalcogenide microwires," *Opt. Lett.* **40**(20), 4687–4690 (2015).
28. G-S Plastic Optics, "Transmission curves," <http://www.gsoptics.com/transmission-curves/>.

## 1. Introduction

The mid-infrared (MIR) range (2–12  $\mu\text{m}$ ) of the optical spectrum is intimately associated with vibrational motion in molecules, enabling many applications related to spectroscopy and chemical sensing [1–3]. Among the approaches utilized to generate MIR light, light sources that depend on nonlinear parametric gain, such as parametric oscillators and supercontinuum (SC) sources raise a great deal of interest due to their broadband operation [4–6]. Parametric processes in a MIR optical source are supported given that the gain medium possesses a sufficiently large nonlinearity coefficient, a good transparency in the MIR, and allows the access to a group velocity dispersion that is close to zero at the pump wavelength.

Chalcogenide (ChG) glasses are such materials compatible with the MIR, covering the spectral range of 1–12  $\mu\text{m}$  for  $\text{As}_2\text{Se}_3$  and the range of 1–8  $\mu\text{m}$  for  $\text{As}_2\text{S}_3$  [7]. ChG glasses are also highly nonlinear media given their intrinsic nonlinear refractive index ( $n_2$ ) up to three orders of magnitude larger than the  $n_2$  of silica glass [8]. Nonlinear effects can also be enhanced from a high-confinement waveguide geometry such as the fiber microwire and the photonic crystal fiber [9,10].

Resulting from the combination of ChG glass and a high-confinement waveguide geometry, ChG microwires are promising components for the fabrication of MIR light sources from parametric processes [11]. With waist diameters at sub-wavelength scale, ChG microwires must be coated to provide mechanical strength and optical insensitivity to environment [12,13].

Hydrogen-based polymers, including PolyMethyl MethAcrylate (PMMA), PolyCarbonate (PC) and Cyclo Olefin Polymer (COP), were successfully used as cladding materials for  $\text{As}_2\text{Se}_3$  microwires [14]. However, the transmission loss of hydrogen-based polymers increases abruptly at wavelengths beyond 1.65  $\mu\text{m}$ , thereby limiting their use. This absorption is caused by molecular resonances at fundamental and overtone transitions of carbon-hydrogen (C-H) bonds [15]. A material free from C-H bonds is thus desirable to avoid the absorption peaks of hydrogen-based polymers and enables optical transmission at wavelengths beyond 1.65  $\mu\text{m}$  and further into the MIR.

An alternative to C-H based polymer is the use of another MIR-transparent ChG glass such as  $\text{As}_2\text{S}_3$  [16]. Unfortunately, the combination of  $\text{As}_2\text{Se}_3$  core with an  $\text{As}_2\text{S}_3$  cladding (or any known ChG-ChG combination) provides a refractive index contrast that is too low to bring the zero dispersion wavelength of a microwire below 3.7  $\mu\text{m}$ , imposing a normal dispersion to all wavelengths  $<3.7 \mu\text{m}$ . As a result, parametric amplification with such compositions cannot be generated from a pump wavelength  $\leq 3.7 \mu\text{m}$ .

In this letter, we use fluorine-based CYTOP as a cladding material for  $\text{As}_2\text{Se}_3$  microwires and demonstrate that CYTOP enables excellent transmission and nonlinear functionalities of the microwire at wavelengths of 1.5  $\mu\text{m}$  up to  $>4.3 \mu\text{m}$ . Not only transmission losses remain low in this wavelength range but also the group-velocity dispersion at these wavelengths can be engineered as normal, anomalous or zero value. We use the high nonlinearity of the CYTOP-cladded microwire to demonstrate multiple orders of four-wave mixing (FWM) and

SC generation. The transparency of CYTOP-cladded microwire is also compared to those of COP- and PMMA-cladded microwires.

## 2. The polymer cladding

Fluorine-based CYTOP (*Asahi Glass*) is a polymer composed of carbon-fluorine (C-F), carbon-carbon (C-C), and carbon-oxygen (C-O) bonds [17]. This differs from widespread hydrogen-based polymers such as COP and PMMA which possess C-H bonds, in addition to C-C and C-O bonds. The transparency in the short MIR wavelengths of a fluorine based polymer versus a hydrogen based polymer is influenced by the presence of C-F bonds rather than C-H bonds. Vibrational wavelengths of a C-F bond are 8.0  $\mu\text{m}$  (1st order) and 4.0  $\mu\text{m}$  (2nd order) whereas the vibrational wavelengths of a C-H bond are 3.4  $\mu\text{m}$  (1st order) and 1.7  $\mu\text{m}$  (2nd order). The vibrational wavelengths of C-C and C-O bonds occur at 8.9  $\mu\text{m}$  (1st order) and 9.1  $\mu\text{m}$  (1st order), respectively, and thus the lowest vibrational wavelength is determined by the presence of C-F or C-H bonds. The fluorine-based polymers thus have absorption peaks at longer wavelengths with respect to the hydrogen-based polymers. Another advantageous property of CYTOP is the low refractive index of 1.33 (at  $\lambda = 1.55 \mu\text{m}$ ), leading to a high refractive index contrast when used to clad an  $\text{As}_2\text{Se}_3$  core. This large refractive index contrast provides flexibility in adjusting the zero dispersion wavelength from the zero dispersion wavelength of bulk  $\text{As}_2\text{Se}_3$  ( $\sim 7 \mu\text{m}$ ) down to the  $\sim 1 \mu\text{m}$ .

The fabrication of optical microwires with ChG core and polymer cladding requires the fulfilling of a few compatibility criterion. First, the polymer cladding must be transparent at the optical wavelengths to be transmitted. Second, the refractive index of the polymer cladding should be as low as possible to ensure a large confinement factor and strong waveguide nonlinearity. Third, the glass transition temperature ( $T_g$ ) and the temperature-dependent viscosity values should be as close as possible to facilitate mechanical compatibility [14]. Table 1 presents glass transition temperature, refractive index and viscosity of  $\text{As}_2\text{Se}_3$ , CYTOP and PMMA.

**Table 1. Glass transition temperature, refractive index ( $\lambda = 1.94 \mu\text{m}$ ) and viscosity ( $T = 210 \text{ }^\circ\text{C}$ ) of  $\text{As}_2\text{Se}_3$ , CYTOP and PMMA.**

	$T_g$ ( $^\circ\text{C}$ )	$n$	Viscosity (Poise)
$\text{As}_2\text{Se}_3$	167 [7]	2.81	$\sim 7.24 \times 10^9$ [18]
CYTOP	108 [17]	1.33	$\sim 1.33 \times 10^5$ [19]
PMMA	104 [20]	1.47	$\sim 2.12 \times 10^5$ [21]

CYTOP is a good material to clad  $\text{As}_2\text{Se}_3$ -based microwires because it provides a significantly improved optical transmission in the MIR wavelengths with respect to hydrogen-based polymers. It also has a lower refractive index than ChG glasses and hydrogen-based polymers, leading to higher refractive index contrast, as well as it is being mechanically compatible with  $\text{As}_2\text{Se}_3$  as required for the microwire fabrication.

## 3. Design

The core diameter and core/cladding composition determine the optical parameters of the microwires: Group-velocity dispersion parameter  $\beta_2$ , waveguide nonlinearity parameter  $\gamma$ , effective mode area  $A_{\text{eff}}$ , and confinement factor  $\Gamma = P_{\text{core}}/P_{\text{total}}$ , where  $P_{\text{core}}$  is the modal power enclosed within the core and  $P_{\text{total}}$  is the total modal power. Those parameters are evaluated from solving the characteristic equation of a cylindrical waveguide with high refractive index contrast and derived from the effective refractive index  $n_{\text{eff}}$ , the propagation constant  $\beta$ , and the electric and magnetic fields distribution E and H of the fundamental  $\text{HE}_{11}$  mode [4]. The waveguide's characteristic equation is solved for a two-layer fiber structure, i.e.  $\text{As}_2\text{Se}_3$  core, CYTOP cladding, as the PMMA coating carries a negligible amount of evanescent power [22].

Figure 1 presents  $\beta_2$ ,  $\gamma$ ,  $\Gamma$  and  $A_{\text{eff}}$  of CYTOP-cladded  $\text{As}_2\text{Se}_3$  microwires as a function of core diameter in the 1.5-4.5  $\mu\text{m}$  wavelength range. The CYTOP-cladded microwire has two zero dispersion wavelengths (ZDW) for a given microwire core diameter, defined  $\text{ZDW}_1$  and

ZDW<sub>2</sub> in order of increasing wavelength. In a practical design, ZDW<sub>1</sub> is generally most useful to increase the gain bandwidth of parametric processes because the dispersion profile around ZDW<sub>1</sub> is flatter than that around ZDW<sub>2</sub>. As well, ZDW<sub>1</sub> provides a larger  $\gamma$  than ZDW<sub>2</sub> in the wavelength range and microwire core diameter of interest. As shown in Fig. 1(c), the mode confinement decreases with increasing wavelengths for a given core diameter, corresponding to an expansion of the guided mode. As shown in Fig. 1(d), this results into an increase of  $A_{\text{eff}}$  and thus more of the mode's evanescent wave propagating into the CYTOP cladding. The attenuation coefficient  $\alpha_{\text{total}}$  arising from light transmission in the microwire is given by  $\alpha_{\text{total}} = \alpha_{\text{As}_2\text{Se}_3} \times \Gamma + \alpha_{\text{polymer}} \times (1-\Gamma)$ , where  $\alpha_{\text{As}_2\text{Se}_3}$  is the attenuation coefficient of As<sub>2</sub>Se<sub>3</sub>, and  $\alpha_{\text{polymer}}$  is the attenuation coefficient of the polymer. The impact of an absorbing cladding is thus reduced when operating the microwire at ZDW<sub>1</sub> rather than at ZDW<sub>2</sub>.

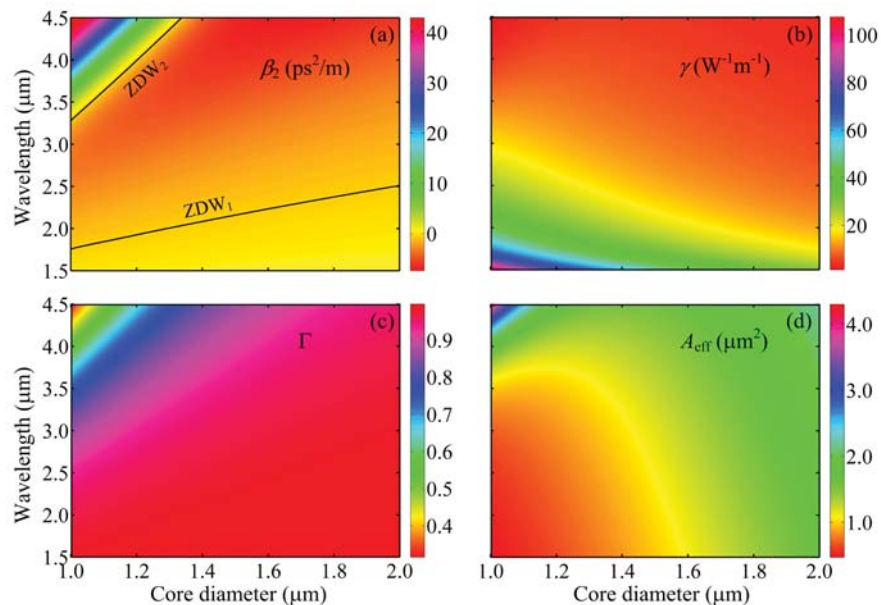


Fig. 1. Optical parameters of CYTOP-cladded As<sub>2</sub>Se<sub>3</sub> microwires as a function of wavelength and core diameter: (a)  $\beta_2$ ; (b)  $\gamma$ ; (c)  $\Gamma$ ; (d)  $A_{\text{eff}}$ .

#### 4. Microwire fabrication

The CYTOP-cladded As<sub>2</sub>Se<sub>3</sub> microwire is fabricated in four steps: Extrusion assembly, *preform* fabrication, *fiber* fabrication and *microwire* fabrication. Figure 2 illustrates the fabrication steps of the fiber. Figure 2(a) shows a schematic of the rod-in-tube method used to make the preform [23]. An As<sub>2</sub>Se<sub>3</sub> rod is placed in a CYTOP tube, then the assembly is placed in a PMMA tube. It is part of our fabrication process to systematically cover preforms of various nature with PMMA to fine-tune the fiber geometry. The As<sub>2</sub>Se<sub>3</sub> rod, CYTOP and PMMA tubes are dried in a vacuum oven prior to the preform fabrication process. Figure 2(b) shows a schematic of the CYTOP-cladded preform fabrication setup, and a photograph of extruded preform. The assembly is fed through an aluminium funnel. Under heat and pressure, the PMMA tube and CYTOP tube shrink and fuse with the As<sub>2</sub>Se<sub>3</sub> rod. The multimaterial composite flows out of the funnel and is pulled at a constant velocity to obtain a uniform preform. Next, the fiber is made by feeding the preform into a drawing funnel heated at controlled temperature. The softened preform is pulled into a fiber with predefined As<sub>2</sub>Se<sub>3</sub> core diameter  $\phi_{\text{As}_2\text{Se}_3}$ , to achieve a maximum coupling efficiency with e.g. SMF-28 fiber. Figure 2(c) shows a schematic of the CYTOP-cladded fiber fabrication setup, a photograph of fiber drawing and a photograph of fiber cross-section. With a cladding to core diameter ratio of 4.2, a microwire with a core diameter of 1.55  $\mu\text{m}$  will allow  $\leq 0.0002\%$  of the evanescent

field power to penetrate the PMMA coating in the 1.5-4.5  $\mu\text{m}$  wavelength range, as estimated from *Lumerical-MODE Solutions*.

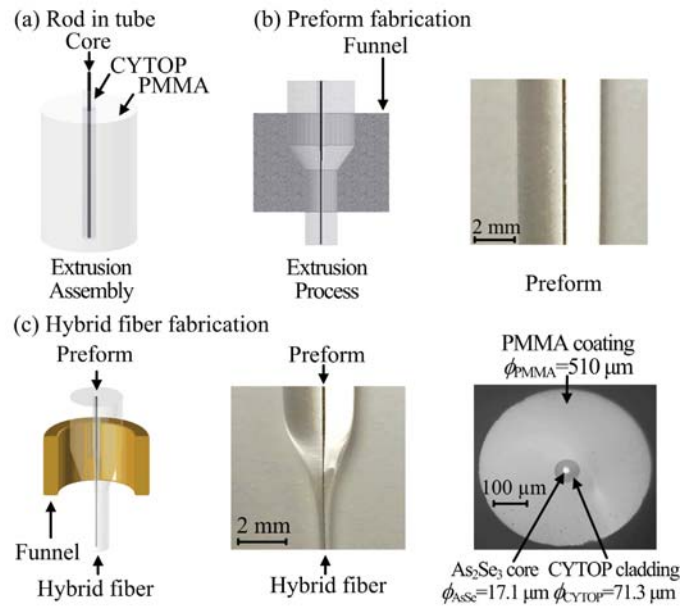


Fig. 2. Fabrication of a polymer-cladded  $\text{As}_2\text{Se}_3$  fiber. (a) Schematic of the rod-in-tube method used to prepare the extrusion assembly. (b) Schematic of the CYTOP-cladded preform fabrication setup (left) and a photograph of extruded preform (right). (c) Schematic of the CYTOP-cladded fiber fabrication setup (left), photograph of fiber drawing (middle) and an optical reflection photograph of cross section (right).

The microwire is fabricated from a sample of fiber tapered using a heat brush method [24], then transferred to a butt-coupling setup. The input end of the microtaper is aligned and connected to SMF-28 fiber using UV-cured epoxy. Figure 3(a) shows the schematic of a microtaper subdivided into fiber, transition and microwire sections. Figure 3(b) is the photograph of a microtaper with wire section length of 5 cm.

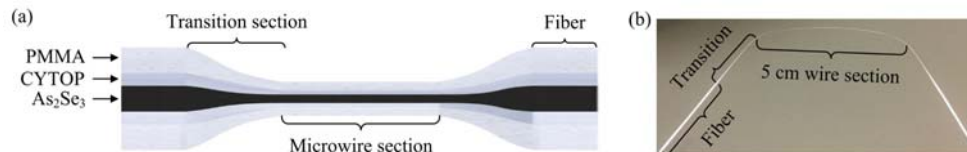


Fig. 3. (a) Schematic of the CYTOP-cladded  $\text{As}_2\text{Se}_3$  microtaper (not to scale). (b) Photograph of a microtaper with wire section length of 5 cm.

## 5. Results and discussion

The transmission loss spectrum of  $\text{As}_2\text{Se}_3$  microwires cladded with CYTOP is investigated experimentally. For the purpose of referencing, the transmittance of microwires cladded with hydrogen-based polymers that are COP 1020R and PMMA is also performed [14]. All microwires studied have a length of 5 cm and modal confinement factor  $\Gamma = 99\%$ . This value of confinement factor is typical for nonlinear parametric processes because it leads to advantageous levels of group-velocity dispersion parameters ( $\beta_2$  and  $\beta_4$ ) while still leading to observable absorption characteristics of the cladding material. To result into  $\Gamma = 99\%$ , the core diameters of CYTOP-, COP- and PMMA-cladded microwires are adjusted to  $\phi_{\text{CYTOP}} = 1.35 \mu\text{m}$ ,  $\phi_{\text{COP}} = 1.48 \mu\text{m}$  and  $\phi_{\text{PMMA}} = 1.46 \mu\text{m}$ . The optical transmission loss of the

microwires is measured at wavelengths in between 1.3  $\mu\text{m}$  and 2.5  $\mu\text{m}$  using a silica-based SC source and an optical spectrum analyzer at either side of the device under test.

Figure 4(a) shows the transmission loss of CYTOP-, COP- and PMMA-cladded  $\text{As}_2\text{Se}_3$  microwires. The microwire with CYTOP cladding is transparent to light at wavelengths up to  $>2.5 \mu\text{m}$ , limited by the spectral range of the spectrum analyzer, without trace of absorption peaks from 1.3  $\mu\text{m}$  to 2.5  $\mu\text{m}$ . Throughout this wavelength range, the transmission loss is stable between 0.11 dB/cm and 0.22 dB/cm. The main source of this uniform loss is the  $\text{As}_2\text{Se}_3$  glass purity, which lies close to the state of the art purity available. In contrast, the COP-cladded microwire reaches a transmission loss of 3 dB at 2.13  $\mu\text{m}$  with traces of two absorption peaks at  $\sim 1.72 \mu\text{m}$  and  $\sim 1.76 \mu\text{m}$  due to the second order vibrational transition of C-H bonds. The transmission loss remains between 0.22 dB/cm and 0.83 dB/cm in the 1.30-2.25  $\mu\text{m}$  range. Finally, the PMMA-cladded microwire reaches a transmission loss of 3 dB at a wavelength of 2.10  $\mu\text{m}$  with traces of an absorption peak at  $\sim 1.65 \mu\text{m}$  due to the second order vibrational transition of C-H bonds. The transmission loss remains between 0.30 dB/cm and 0.83 dB/cm from 1.30  $\mu\text{m}$  to 2.20  $\mu\text{m}$ . The transmission loss of the CYTOP-cladded microwire is therefore substantially decreased with respect to COP- and PMMA-cladded microwires, especially at wavelengths in excess of 1.65  $\mu\text{m}$ .

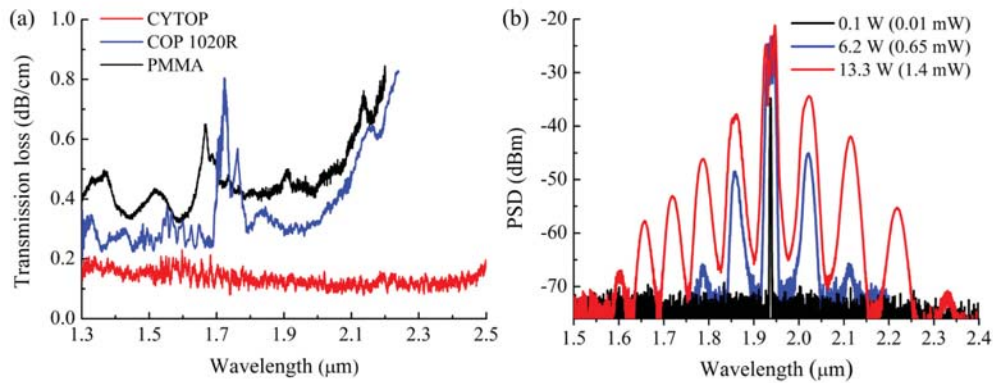


Fig. 4. (a) Transmission loss spectra of CYTOP-, COP 1020R-, and PMMA-cladded  $\text{As}_2\text{Se}_3$  microwires; (b) nonlinearly broadened spectra of CYTOP-cladded  $\text{As}_2\text{Se}_3$  microwire at various pump powers. The legend presents corresponding coupled peak (average) powers.

Nonlinear parametric processes in a CYTOP-cladded  $\text{As}_2\text{Se}_3$  microwire are also investigated. The microwire has a length  $L_w = 5 \text{ cm}$  and core diameter  $\phi = 1.35 \mu\text{m}$ , leading to  $\gamma = 27 \text{ W}^{-1}\text{m}^{-1}$ ,  $\beta_2 = -0.273 \text{ ps}^2/\text{m}$  and  $\beta_4 = -1.17 \times 10^{-5} \text{ ps}^4/\text{m}$ . The transmission loss of the microwire is 0.15 dB/cm at a wavelength of 1.94  $\mu\text{m}$ . Pump pulses centered at a wavelength of 1.94  $\mu\text{m}$  with a duration of 3.5 ps after pulse shaping by a band-pass filter are launched into the microwire. Figure 4(b) shows spectra collected at the output of the microwire. As the coupled pump peak (average) power is increased up to 13.3 W (1.4 mW), side lobes of increasing power are observed along with spectral broadening of the pump signal. The nonlinear processes observed include self-phase modulation of the pump, but also Raman enhanced FWM [4]; itself mixing with the pump to provide several orders of degenerate FWM.

SC generation in a CYTOP-cladded  $\text{As}_2\text{Se}_3$  microwire is also investigated. The design includes a microwire with a length of  $L_w = 10 \text{ cm}$  and  $\phi = 1.55 \mu\text{m}$ , leading to  $\beta_2 = -0.04 \text{ ps}^2/\text{m}$ ,  $\beta_3 = 0.003 \text{ ps}^3/\text{m}$ ,  $\beta_4 = -0.09 \times 10^{-4} \text{ ps}^4/\text{m}$  and  $\gamma = 21 \text{ W}^{-1}\text{m}^{-1}$ . The butt-coupling loss from SMF-28 fiber to the hybrid fiber is 1.1 dB, including 0.5 dB of Fresnel reflection loss at the fiber's interface, and the rest due to mode-mismatch losses. Pump pulses centered at 1.94  $\mu\text{m}$  with a duration of 3.0 ps are launched into the microwire and analyzed using a Fourier Transform Infrared Spectrometer (FTIR). As pump pulses are launched into the microwire, modulation instability triggers the SC generation, breaking the input picosecond pulses into

femtosecond sub-pulses, followed by soliton dynamics [25]. Figure 5(a) shows experimentally measured spectra as a function of the coupled pump power up to 1044 W (100 mW) in peak (average) power. A SC is generated, spanning from 1.0  $\mu\text{m}$  to 4.3  $\mu\text{m}$  at  $-30$  dB relative to the peak value. A dip within the SC spectrum in the 2.5-3.0  $\mu\text{m}$  spectral range could be caused by low pressure water vapour inside the FTIR [26]. The limited extent of the SC at wavelengths beyond 4.3  $\mu\text{m}$  is expected to be caused by absorption from the second order vibrational overtone of the C-F bond in CYTOP. Take note that the microwire length of 10 cm was chosen to emphasize the absorption features in the microwire and that a microwire of a few millimeters would provide sufficient nonlinearity and dispersion for SC generation with a reduced absorption signature by the cladding [27].

At last, SC generation is compared for CYTOP- and COP-cladded microwires with core diameters of 1.55  $\mu\text{m}$  and 1.59  $\mu\text{m}$ , respectively. Those core diameters were chosen as they both lead to  $\beta_2 = -0.04$  ps<sup>2</sup>/m at the pump wavelength of 1.94  $\mu\text{m}$ . Both microwires are 10 cm long and pumped at 1044 W (100 mW) in peak (average) power. Figure 5(b) shows the resulting SC spectra. The SC spectrum of COP-cladded microwire is limited to 2.3  $\mu\text{m}$  due to the strong absorption features of this hydrogen-based polymer, as observed in Fig. 4(a) [28].

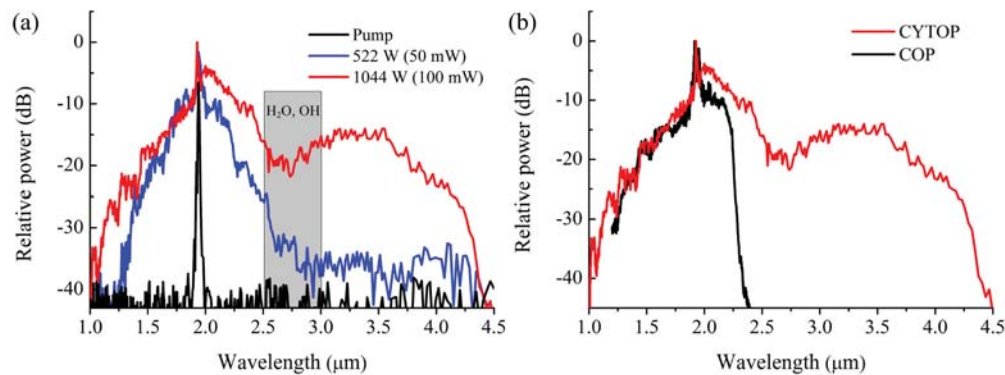


Fig. 5. (a) SC spectra at various coupled pump powers for a CYTOP-cladded microwire with an As<sub>2</sub>Se<sub>3</sub> core diameter of 1.55  $\mu\text{m}$ . (b) SC spectra of CYTOP- and COP-cladded microwires at a peak (average) pump power of 1044 W (100 mW).

## 6. Conclusion

We have shown that CYTOP preserves the linear and nonlinear functionalities of As<sub>2</sub>Se<sub>3</sub> microwires at wavelengths from 1.3  $\mu\text{m}$  up to  $>4.3$   $\mu\text{m}$ . The CYTOP cladding significantly improves the transmission bandwidth with respect to hydrogen-based polymer claddings, especially at wavelengths above 1.65  $\mu\text{m}$ . The CYTOP-cladded microwire has an engineerable group-velocity dispersion in the 1-7  $\mu\text{m}$  wavelength range, enabling anomalous, normal, or zero dispersion. For the SC generation demonstrations, the microwire length of 10 cm was chosen to emphasize the absorption features in the microwire. In practice, a microwire design of a few millimeters would provide sufficient nonlinearity and dispersion for SC generation with a reduced absorption signature by the cladding.

## Funding

The Collaborative Research and Development Program of the Natural Sciences and Engineering Research Council of Canada (NSERC).

## Acknowledgment

The authors are thankful to Coractive High-Tech for providing the chalcogenide glass used in the experiments.